Utilization of Matched Pulses to Improve Fault Detection in Wire Networks

Layane ABBOUD [#1], Andrea COZZA [#2], Lionel PICHON [*3]

[#] *Département de Recherche en Électromagnétisme*
SUPELEC, 3 rue Joliot-Curie, 91192 Gif-sur-Yvette, France
[1] Layane.Abboud@supelec.fr
[2] Andrea.Cozza@supelec.fr

[*] *Laboratoire de Génie Électrique de Paris,*
LGEP - CNRS / SUPELEC - 91192 Gif-sur-Yvette, France
[3] Lionel.Pichon@supelec.fr

***Abstract*—A new concept to fault detection in wire networks, based on the properties of time reversal, is presented. The method, called the Matched Pulse approach (MP), propose to adapt the testing signal to the analyzed network, instead of using a predefined signal, as opposed to existing reflectometry methods. Through mathematical study and numerical simulations, we show the benefits of this technique. A physical interpretation is also presented to better understand the proposed approach.**

***Index Terms*—wire networks, fault detection, time reversal.**

I. Introduction

Location of faults on wires has become an area of international concern [1]. Wired networks can be found everywhere: in transportation systems, industrial machinery, buildings, nuclear facilities, power distribution systems, etc., so that faulty electrical wiring has been considered among the most significant potential cause of failure and maintenance cost in these structures [2].

Away from the classical methods of wire testing such as visual inspection and impedance testing [1], reflectometry methods are widely used today to help detecting and locating wire faults. The basic concept of these methods is presented in the next section. Generally, hard faults (open and short circuits) are detectable through reflectometry, while soft faults (damaged insulation, etc.) are more critical to detect, especially in complex wire networks.

In this paper, we propose an approach to fault detection in wire networks, called the Matched Pulse approach (MP). This proposed method relies on the idea of adapting the testing signal to the wire network to be analyzed, instead of injecting a predefined testing signal, as opposed to reflectometry methods. This method will be shown to be always beneficial when compared to standard Time Domain Reflectometry (TDR) [3], as it permits to increase the detection probability of the fault, especially when it comes to identifying soft faults.

The paper is organized as follows: in the next section we give a brief reminder of the principle of reflectometry methods, then in the third section introduce the MP approach, based on the matched filter principle. The fourth and fifth sections present the investigation tools we used for comparing the MP and TDR approaches : by first defining an echo-energy gain, followed by a parametric study which shows the benefits of the new approach. This mathematical study is followed by a physical interpretation of the obtained results, based on the properties of time reversal [4].

II. Reflectometry Methods

Reflectometry methods are widely used today for fault detection and location. These methods send testing signals down the wire network to be analyzed. They include TDR, which uses a fast rise time step or pulsed signal as the testing signal, Frequency Domain Reflectometry [5] which uses multiple sinusoidal signals, Sequence TDR [6] which uses pseudo noise, and Spread Spectrum TDR which uses pseudo noise modulated onto a sinusoidal carrier signal. Several other methods also exist, such as Noise Domain Reflectometry [7], Mixed Signal Reflectometry [8], etc. However, the principle of these methods remains the same: we first inject a predefined signal into the system to be examined, and then we analyze the reflected signal. The first step in the analyzing process is to decide whether or not a fault exists; this is the detection phase, where the reflected signal is analyzed to try to determine the echo from an eventual fault. Once detected, the second step is to determine the position and nature of this fault.

As we already mentioned, hard faults are easily detected using reflectometry methods, while soft faults are generally not. Additional complexity arises when using wire networks, because faults can be masked by the presence of several reflection sources (such as junctions, branches, mismatched loads, etc.); this produces multiple echoes, making it difficult to identify the one corresponding to the actual fault. Furthermore, those same reflections disperse the energy of the interesting echo and make the detection process even more difficult.

The problem of fault detection in wire networks can be compared to the problem of target detection encountered in radar, when the target to be detected is embedded in a cluttered medium [9]. In order to enhance the probability of detection of the target and reduce the false-alarm rate, the idea is to maximize the energy of the echo from the target to be detected, thus increasing its signal to noise ratio. Such approach has

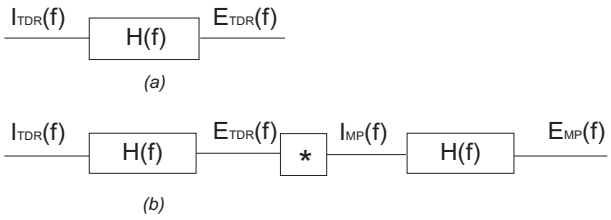

Fig. 1. Comparison of the TDR and MP methods: (a) is the TDR block diagram, and (b) is the MP one.

been studied in [4] [10], by exploiting the properties of time-reversal.

In this paper, we introduce the MP approach, based on Time Reversal techniques, and compare it with the classical TDR. The analyzing method is the following: we will consider that the testing signal (i.e., the injected signal) is the input to our system, and the reflected signal is the output; the transfer function of this system in the absence of the fault is denoted as $H_0(f)$ and in the presence of the fault is $H_F(f)$. Generally, we can either analyze the reflected signal directly [3], or take the difference of the two reflected signals (with and without the fault), especially when considering soft faults [11], so that the echo from the fault would be more easily detected. this latter method is the one we will be using, assuming that our system is linear time invariant. Analyzing the difference of the two reflected signals is consequently equivalent to analyzing the output of an equivalent system whose transfer function $H(f)$ is defined as follows

$$H(f) = H_F(f) - H_0(f) \tag{1}$$

This equivalent system will be referred to as the difference system.

III. Matched Pulse

In this section we introduce the basic concept of the MP approach. Instead of injecting a predefined signal into the network to be analyzed, as for existing reflectometry methods, the idea is to adapt the injected signal to the system, so that the energy of the echo from the fault is maximized, thus increasing its detection probability. Such a tailor-made signal, or MP, can be synthesized considering the matched filter approach used in signal processing [12]. According to this theory, a matched filter is obtained by correlating a known signal, or template, with an unknown signal to detect the presence of the template in the unknown signal. This is equivalent to convolving the unknown signal with a time-reversed version of the template. The matched filter is the optimal linear filter for maximizing the signal to noise ratio (SNR) in the presence of additive white noise.

By examining Figure 1, the same idea is encountered. Let us remind that the testing signals are $I_{TDR}(f)$ and $I_{MP}(f)$, and $H(f)$ is the transfer function. In the TDR scheme, we simply have the predefined signal injected into the system, thus resulting in the echo $E_{TDR}(f)$. As for the MP, if we consider for example that we are injecting a Dirac Pulse (in the time domain), then the TDR echo would be the transfer function of the system. By sending the time reversed version of this echo into the same system, we are effectively auto correlating it. This is the same as doing the matched filtering of the TDR echo to obtain the MP echo $E_{MP}(f)$. Therefore we have a higher efficiency in the MP case, because the signal is adapted to the studied system. This fact will also be shown in section V.

IV. Simulation Setup

In order to better illustrate the effects of introducing the MP approach, we chose to compare it with the TDR. The simulation method and analyzed configuration are presented in this section.

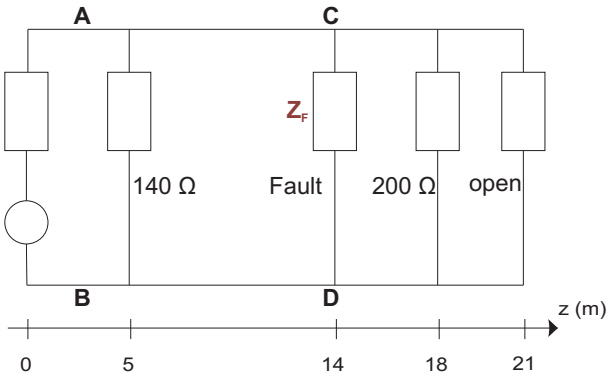

Fig. 2. The equivalent wire network analyzed in this paper.

A. Analyzed Configuration

The configuration we chose to study is represented in Figure 2. It consists of a lossless transmission line with a $75\ \Omega$ characteristic impedance, as for coaxial cables. The line is terminated by an open circuit at its far end. Two parallel impedances of, respectively, $140\ \Omega$ and $200\ \Omega$, stand for equivalent loads, such as for two further parallel branches. The fault to be detected is located between those two impedances. We chose to study such a configuration as it is difficult in practice to analyze it with the existing reflectometry methods, due to the number of echoes resulting from the network discontinuities. The fault to be detected is modeled as a parallel impedance. In this paper we will only examine such types of faults.

B. Simulation Method

We used the transmission line theory as presented in [13]. Briefly, let us consider a uniform scalar transmission line, as illustrated in Figure 3; V_S is the injected voltage, and Z_S is the impedance of the source, considered equal to the characteristic impedance of the line Z_c. The impedance of the load at the end of the line is denoted as Z_L. The voltage and current at any point of the line which position is z can be calculated according to the following formulas:

$$V(z) = V_0^+ \exp(-j\gamma z) + V_0^- \exp(j\gamma z) \tag{2}$$

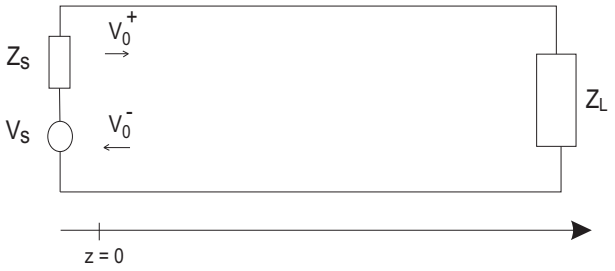

Fig. 3. A model illustrating the transmission line theory used in the paper: V_0^+ and V_0^- are the modal variables to be determined in order to characterize the voltage and current propagation along the line.

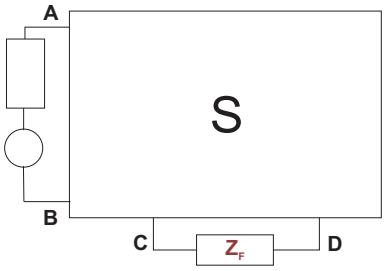

Fig. 4. The equivalent illustration of the analyzed network, used in the simulations.

$$I(z) = I_0^+ \exp(-j\gamma z) - I_0^- \exp(j\gamma z) \tag{3}$$

V_0^+ and V_0^- are the modal voltages in the frequency domain, and I_0^+ and I_0^- are the modal currents. γ is the propagation constant. We can write: $Z_c = V_0^{\pm}/I_0^{\pm}$. In order to determine the voltage and current at any point of the line, we need to determine the values of two modal variables. The advantage of this method is therefore obvious: we have a full description of the evolution of the voltage and current along the transmission line just by obtaining the values of two modal variables, which can be determined by imposing the boundary conditions at the source and the load. The fact that this analytic model describes physical phenomenons made it interesting to use in our software implementation.

V. Gain of the Normalized Echo Energies of the MP and TDR Approaches

In order to test the ability of the proposed method in delivering higher echo energies, we now introduce the tools we used to compare the MP and TDR approaches. This is followed by a parametric study and numerical simulations that prove the advantages of our new approach.

A. Definition

We will first define a gain $G(Z_F)$ as the ratio of the normalized energy of the MP echo to the normalized energy of the TDR echo. We note that the normalization is done according to the energy of the testing signal in each case, that is the normalized energy of the TDR echo is the ratio of the energy of this echo to the energy of the gaussian pulse, and the normalized energy of the MP echo is the ratio of the energy of this echo to the energy of the TDR echo (which is the time reversed version of the testing signal in this case). This normalization makes possible the comparison of the two methods.

The normalized energy of the TDR echo is

$$\mathcal{E}_{\mathrm{TDR}}(f) = \frac{\int |E_{TDR}|^2 \mathrm{d}f}{\int |I_{TDR}|^2 \mathrm{d}f} = \frac{\int |H(f)|^2 |I_{TDR}(f)|^2 \mathrm{d}f}{\int |I_{TDR}|^2 \mathrm{d}f} \tag{4}$$

and the normalized energy of the MP echo is

$$\mathcal{E}_{\mathrm{MP}}(f) = \frac{\int |E_{MP}|^2 \mathrm{d}f}{\int |I_{MP}|^2 \mathrm{d}f} = \frac{\int |H(f)|^4 |I_{TDR}|^2 \mathrm{d}f}{\int |H(f)|^2 |I_{TDR}|^2 \mathrm{d}f} \tag{5}$$

The gain is the ratio of these normalized energies, therefore we can write

$$G(Z_F) = \frac{\mathcal{E}_{\mathrm{MP}}(f)}{\mathcal{E}_{\mathrm{TDR}}(f)} \tag{6}$$

Using the Cauchy-Schwartz inequality [12], one can easily prove that $G(Z_F)$ is always greater than 1, and consequently the MP approach is always beneficial compared to TDR.

B. Parametric Study

We analyze the previously defined gain in terms of the nature and position of the fault. But first, it is interesting to be able to predict the variation of the gain according to the nature of the fault. Therefore, we chose to express this gain in terms of the reflection coefficient from the fault Γ_F, and the scattering matrix S of a two ports system. This representation would allow us, for a single numerical characterization (corresponding to a given network configuration), to directly predict the system's response for any fault impedance Z_F.

To better illustrate this idea let us examine Figure 4. We considered the setup of Figure 2. The system is described by the scattering matrix S, linking its inputs to its outputs: the inputs are the incident voltage waves from the two ports, and the outputs are the reflected waves. The impact of introducing a fault to the system is described by Γ_F. The transfer function of the system may now be written as follows

$$H(f) = \frac{S_{12}S_{21}(1-\Gamma_F)}{(1-S_{22})(1-\Gamma_F S_{22})} \tag{7}$$

By introducing this expression into Equation (6), we can predict how the gain changes according to the impedance value of the fault, in the previously illustrated configuration (see Figure 2).

C. Numerical Results

We consider the numerical results obtained by changing the value and position of the fault in the system illustrated in Figure 2, and computing the corresponding value of $G(Z_F)$. In our experiment, we consider that the impedance value of

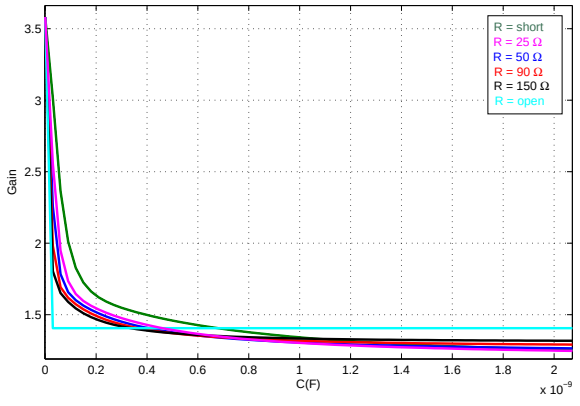

(a)

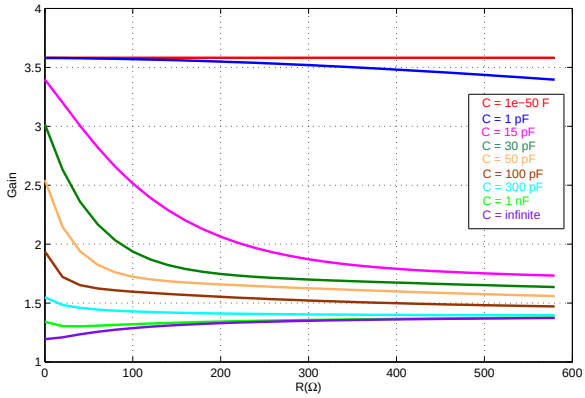

(b)

Fig. 5. The values of $G(Z_F)$ in terms of the impedance of the fault, for several values of R (a) and C (b). The studied system is illustrated in Figure 4.

the fault is expressed as

$$Z_F = R + \frac{1}{j\omega C} \tag{8}$$

where R is the real part and $-1/\omega C$ the imaginary one. The values of this impedance are chosen in order to simulate as much as possible the real faults [11]. The values of $G(Z_F)$ in terms of R and C are shown in Figures 5a and 5b. By examining the gain's variation in the two figures, we can see that for very small values of the capacitance, the value of the gain is about 3.5. Note also that in this case, the value of R does not have a big influence on $G(Z_F)$, and consequently the softness or hardness of the fault does not affect the gain. As the capacitance increases, the gain decreases around 1.2 for a big value of C. Furthermore, when closely examining those results, we can notice that it is the constant $\tau = RC$ which influences the most $G(Z_F)$. When the value of $1/\tau$ (i.e., the cutoff frequency of Z_F) starts to reduce the bandwidth of the injected signal, the gain starts to decrease. This fact is not similar to the one we will be examining in Figure 7, because in this case the injected energy is still the same, but the bandwidth of the echo is reduced due to the interactions

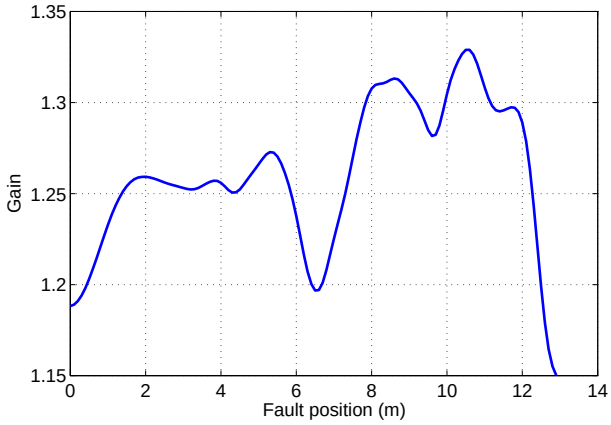

Fig. 6. The values of $G(Z_F)$ in terms of the fault's position. The studied system is represented in Figure 2. The fault is being moved from the 140 Ω impedance towards the 200 Ω impedance.

with the loads. Here it is also important to note the effect of the dispersion introduced by the presence of the capacitance C: when its value increases, the gain decreases; In fact the state equation of reactive elements does not meet the requirement of having a time reversible system, unlike the equation of the wave propagation. Therefore the dispersion introduced by such an element would result in decreasing the effectiveness of the time reversal operation, which corresponds to decreasing the value of $G(Z_F)$.

The next step is to observe the variation of $G(Z_F)$ according to the variation of the fault's position. In our case we considered the previously studied configuration, and limited the variation of the fault's position between the two impedances (which values are 140 Ω and 200 Ω). The origin of the position is the 140 Ω impedance, and the fault is being moved toward the other impedance. We chose an arbitrary value of the fault, where $R = 50$ Ω and $C = 1$ nF. The numerical results are shown in Figure 6, where it is clear that the position of the fault influences the gain $G(Z_F)$, keeping the advantage of the MP over the TDR. Note that the values of the gain change within 1.329 and 1.15. We notice that $G(Z_F)$ decreases to reach its lowest values when the fault is close to the 140 Ω and 200 Ω impedances. In these cases, we lose the multiple reflections, which will eventually decrease the efficiency of the time reversal process.

Another interesting aspect is to observe the influence of the bandwidth of the injected signal on $G(Z_F)$. Here, we remind that the choice of the sampling step directly affects the resolution capacity of the TDR.

According to Equation (6), it is obvious that the bandwidth of the testing signal limits the integration interval, and also the spectrum of the injected signal plays the role of a weighting function for the transfer function of the difference system. Given that the theoretical prediction of the influence of this variation is difficult, we computed the values of $G(Z_F)$ in terms of the bandwidth of the injected signal, for the same

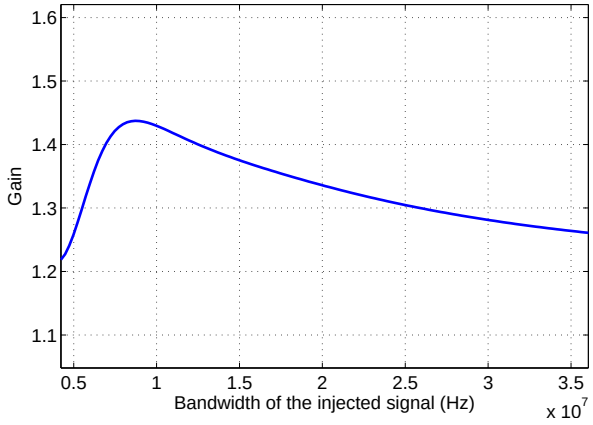

Fig. 7. The Gain $G(Z_F)$ in terms of the bandwidth of the injected gaussian pulse. The system is the same as illustrated in Figure 2.

given value of Z_F ($R = 50\ \Omega$ and $C = 1$ nF). The results are shown in Figure 7. We can notice that while increasing the bandwidth of the injected signal, we are averaging the integrand, so after a certain bandwidth (about 35 MHz in our example of Figure 7) the gain's value gets steadier. Note that we are not able to predict the optimal value of the bandwidth because it is directly related to the transfer function $H(f)$.

VI. Study of a Particular Case

In this section we focus on a particular case where the fault is soft, in order to observe and compare the injected and received signals in the TDR and MP cases, keeping the same configuration as before (see Figure 2). If we observed the equivalent scheme of Figure 4, we will notice that a soft fault can be modeled by a small variation of the reflection coefficient compared to the case where the fault doesn't exist. In other words, a value of the fault close to the case where we have an open circuit. The value we chose is $600\ \Omega$, and consequently $|\Gamma_F| = 0.059$. Thus, we have a very small reflection on the fault.

A. Testing Signals and Echoes

Let us examine Figure 8a. The testing signal in the TDR method is a gaussian pulse. In the MP case, the testing signal is the time reversed version of the TDR echo. The two testing signals are normalized to the same energy. We can notice the shape of the testing signal in the MP case, containing the information from the analyzed system; the different echoes with positive and negative peaks finally contribute to maximize the energy of the echo from the fault to be detected. This will be observed in the next section. We also notice that the highest peak has its amplitude lower than the amplitude of the gaussian pulse, a fact that might be useful when examining electromagnetic interference problems.

As for the echoes obtained in both cases, they are shown in Figure 8b. It is clear that the highest peak of the MP echo is greater than the TDR one, thus increasing the detection probability of the fault. It is also observable that the ratio

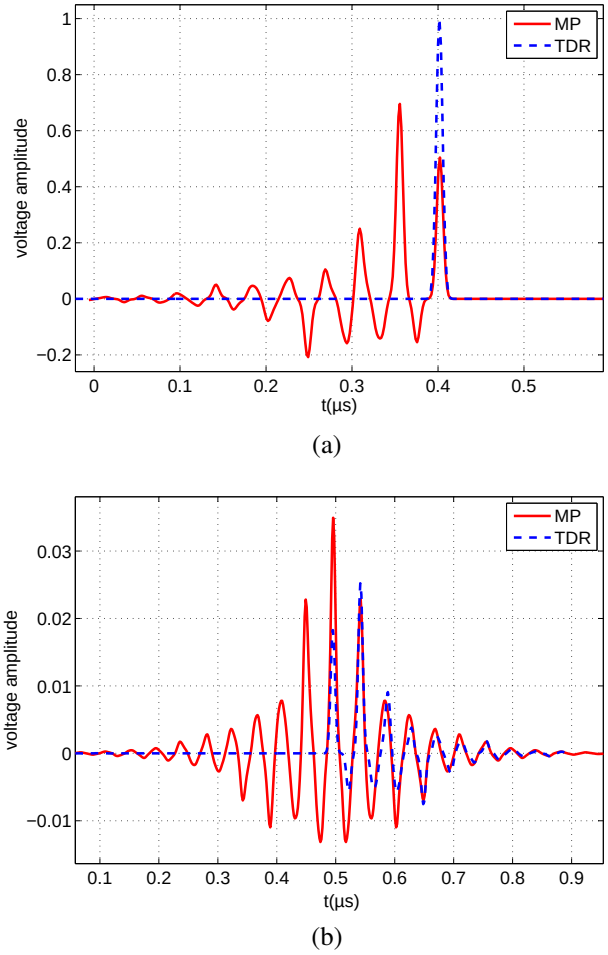

Fig. 8. The injected signals in the TDR and MP cases, normalized to the same energy (a); The echoes obtained in both cases (b). The system is the same as illustrated in Figure 2.

of the amplitude of the highest peak to the amplitude of the secondary peak is greater in the MP case (about 1.532 in the MP case compared to 1.379 in the TDR case); this is important because it reduces the ambiguity of detection in the case of multiple echoes. Further discussion is presented in the next section, when examining the propagation of the two echoes.

B. Physical Interpretation

To better understand physically the reason why the MP approach results in a higher efficiency, we first illustrate the propagation of the echoes in the TDR and MP cases, according to the diagrams of Figures 9a and 9b. Those diagrams represent the propagation of the voltage along the transmission line, both in space (horizontal axis) and time (vertical axis). The testing signals are normalized to the same energy. Here we considered the difference system, so that is equivalent to subtracting the reflected signals obtained with the presence and absence of the fault. The obtained signals contain the information from the fault to be detected. The three vertical black lines indicate respectively the positions of the three impedances: the $140\ \Omega$

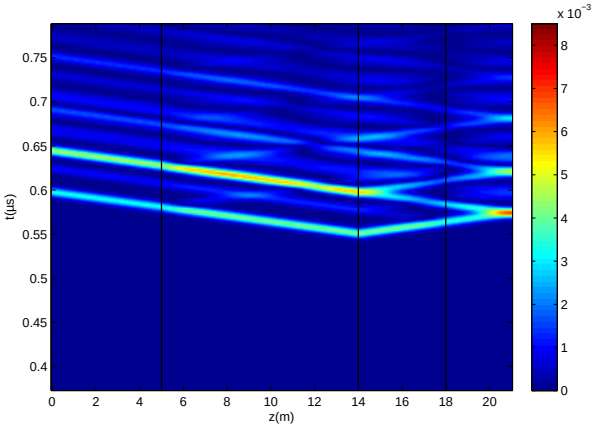

(a)

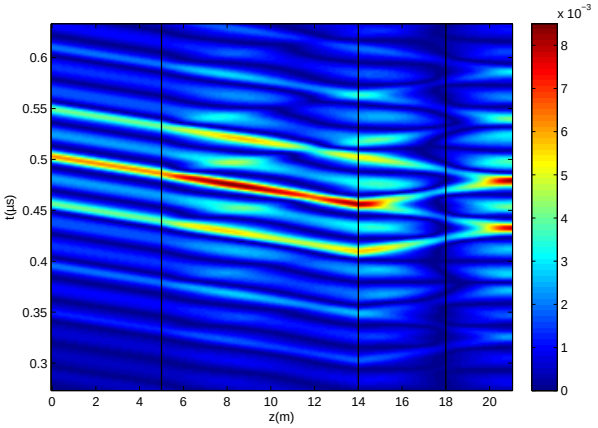

(b)

Fig. 9. The Space-Time diagram of the TDR echo showing its propagation in the system illustrated in Figure 2 (a); The Space - Time diagram of the MP echo (b).

impedance, the fault, and the 200 Ω impedance.

In the TDR case, we observe that the echo from the fault to be detected results mainly from the reflection of the testing signal on the fault. We should note that the testing signal is not seen on the diagram at the injection time, because it is the same with and without the fault; the subtraction of the reflected signals thus eliminate it. In the MP case, there is an increasing number of echoes compared to TDR, due to the shape of the testing signal; those echoes contribute to maximize the energy from the fault to be detected, as we can observe in Figure 9b at the fault's position: we can notice that in the TDR case, in the first reflection on the fault, the energy is almost equally distributed to the left and to the right of the fault, while in the MP case the energy is much more concentrated to the left of the fault (i.e., to the source side where we receive the echo). The echoes obtained in Figure 8b can be verified by looking at the position $z = 0$ in the two diagrams, along the time axis. We can observe the origins of the highest peaks in both cases. Also note that the 140 Ω impedance reduces the energy of the echo, as observed in the two diagrams, while the 200 Ω impedance is high enough not to significantly affect the echo propagation.

The results we observed in the case of the MP are due to the properties of time reversal. The Time Reversal is a self adaptive technique that compensates for the distortions due to the propagation through inhomogeneous media, in other words it takes into account the information recorded from the medium thus resulting in a higher efficiency. When we examined the previously studied diagrams, we saw how we used the TDR echoes (normally a nuisance in fault detection) to obtain an echo with a higher energy in the MP case. The Time Reversal allowed to synchronize these echoes, and thus made it possible to maximize the energy of the MP echo. This was not observed in the TDR case, where the reflected signal only takes into account the time delay to the fault.

VII. Conclusion

This paper presented an approach to fault detection in wire networks, based on the properties of time reversal: the Matched Pulse approach. This method was compared to the classical Time Domain Reflectometry, through mathematical analysis where we defined and studied a gain in order to show the benefits of this approach. The MP was found to be always beneficial compared to TDR, as it permits to increase the detection probability of the fault to be detected. A physical interpretation based on the properties of time reversal allowed us next to better understand the proposed method.

References

[1] C. Furse and R. Haupt, "Down to the wire," *IEEE Spectrum*, vol. 38, no. 2, pp. 34–39, 2001.

[2] "Review of federal programs for wire system safety," National Science and Technology Council, White House, Final Report, Nov. 2000.

[3] C. Furse, Y. C. Chung, C. Lo, and P. Pendayala, "A critical comparison of reflectometry methods for location of wiring faults," *Smart Structures and Systems*, vol. 2, no. 1, pp. 25–46, 2006.

[4] M. Fink, "Time reversed acoustics," *Scientific American*, pp. 91–97, November 1999.

[5] C. Furse, Y. C. Chung, R. Dangol, M. N. G. Mabey, and R. Woodward, "Frequency-domain reflectometery for on-board testing of aging aircraft wiring," *IEEE Transactions on Electromagnetic Compatibility*, vol. 45, no. 2, pp. 306–315, May 2003.

[6] P. Smith, C. Furse, and J. Gunther, "Analysis of spread spectrum time domain reflectometry for wire fault location," *IEEE Sensors Journal*, vol. 5, no. 6, pp. 1469–1478, December 2005.

[7] C. Lo and C. Furse, "Noise-domain reflectometry for locating wiring faults," *IEEE Transactions on Electromagnetic Compatibility*, vol. 47, no. 1, pp. 97–104, Feb. 2005.

[8] P. Tsai, C. Lo, Y. C. Chung, and C. Furse, "Mixed-signal reflectometer for location of faults on aging wiring," *Sensors Journal, IEEE*, vol. 5, no. 6, pp. 1479–1482, Dec. 2005.

[9] Y. Jiang, D. Stancil, and J.-G. Zhu, "Antenna array detection in highly cluttered environment using time reversal method," in *Microwave Symposium, 2007. IEEE/MTT-S International*, June 2007, pp. 1731–1734.

[10] M. Fink, "Time reversal of ultrasonic fields - part 1: basic principles," *IEEE Transactions on Ultrasonics, Ferroelectrics, and Frequency Control*, vol. 39, no. 5, pp. 555–566, September 1992.

[11] L. Griffiths, R. Parakh, C. Furse, and B. Baker, "The invisible fray: a critical analysis of the use of reflectometry for fray location," *Sensors Journal, IEEE*, vol. 6, no. 3, pp. 697–706, June 2006.

[12] A. Papoulis, *Signal Analysis*. McGraw-Hill, 1977.

[13] C. R. Paul, *Analysis of Multiconductor Transmission Lines*, K. Chang, Ed. Wiley-Interscience, 1994.